Bose-Einstein condensation of positronium in silica pores

O. Morandi, P.-A. Hervieux, and G. Manfredi
Institut de Physique et Chimie des Matériaux de Strasbourg, CNRS and University of Strasbourg, 23 rue du Loess, F-67034 Strasbourg, France

(Received 10 June 2013; revised manuscript received 24 January 2014; published 6 March 2014)

We investigate the possibility to produce a Bose-Einstein condensate made of positronium atoms in a porous silica material containing isolated nanometric cavities. The evolution equation of a weakly interacting positronium system is presented. The model includes the interactions among the atoms in the condensate, the surrounding gas of noncondensed atoms, and the pore surface. The final system is expressed by the Boltzmann evolution equation for noncondensed particles coupled with the Gross-Pitaevskii equation for the condensate. In particular, we focus on the estimation of the time necessary to form a condensate containing a macroscopic fraction of the positronium atoms initially injected in the material. The numerical simulations reveal that the condensation process is compatible with the lifetime of ortho-positronium.

DOI: 10.1103/PhysRevA.89.033609 PACS number(s): 03.75.Hh, 05.30.Jp, 36.10.Dr, 51.10.+y

I. INTRODUCTION

At low density and temperature, positrons and electrons can form a bound state known as "positronium," which behaves effectively as a light neutral atom with physical properties similar to those of hydrogen. However, being composed of matter and antimatter, positronium is an unstable atom with a finite lifetime, as the electron and the positron have a certain probability to annihilate. In its ground state, positronium consists of triplet states (ortho-positronium, with a lifetime equal to 142 ns) and a singlet state (para-positronium, with lifetime 125 ps). One of the simplest processes devised for the production of a gas of positronium relies on the implantation of highly energetic positrons in a solid. Using modern techniques, it is possible to generate collimated beams of positrons and to direct them on very small spots, with a diameter of the order of 100 μm [1]. At a certain distance (typically around 100 nm) from the surface of the solid target, the positrons are likely to capture an electron from the solid and form a positronium atom. When the positrons are injected into a porous material, the positronium atoms are easily trapped inside the cavities. Thus, it has been suggested that a Bose-Einstein condensate (BEC) made of positronium could be created by trapping a sufficiently dense positronium gas inside such small cavities [2].

Using state-of-the-art positron-production technology, one can obtain positronium gases with a density that is around two orders of magnitude too low to achieve condensation [3]. The creation of a positronium gas with density of 10^{-3} nm^{-3} is under experimental investigation and may soon be reached [4]. Due to the low mass of the positronium atom, at a density of 10^{-3} nm^{-3} (10^{-2} nm^{-3}) the critical temperature for BEC formation is $T_c = 14$ K ($T_c = 66$ K).

Films of porous silica have been successfully employed for the detection of the quenched lifetime of positronium, as well as for the creation of excited atomic states and the dipositronium molecule Ps_2. [5–7]. The main challenge towards the creation of a BEC of positronium in a porous material concerns the time needed to cool down the gas trapped in the cavities. Indeed, the lifetime of positronium atoms is not sufficiently long to ensure that the condensation process can be completed before the annihilation of all the atoms of the gas.

Several authors have studied the evolution of the temperature of positronium gases in aggregates of silica aerogel and silica powder [8–10]. Measurements performed by the group of Takada indicate that the time necessary for the full positronium thermalization is around 10 ns for pores with a radius of 5 nm [8]. However, quantum confinement effects could affect the thermalization time in the case of very small pores. In particular, for samples containing pores with a radius of 2.7 nm, no thermalization was observed [11]. The reason was ascribed by the authors to the quantization of the energy levels in the cavity. In small volumes, the number of available energy levels for the positronium atoms is reduced and the gas cannot reach the temperature of the silica sample [12]. In the present contribution, we shall focus on pores larger than 100 nm, for which the quantization effect on the temperature evolution is negligible. Moreover, the geometrical arrangement of the pores affects the efficiency of the material to trap and cool the positronium atoms. Nowadays, it is possible to produce well-defined pore structures of controlled size. For instance, in [13] it was shown that inside a material containing cylindrical nanochannels of diameter in the range of 5–8 nm, the positronium atoms thermalize at the temperature of 150 K, in a time shorter than 15–20 ns.

Due to the high implantation energy of the positron, the positronium gas is created in the pores with an initial energy around 0.4–3 eV, which is far above the critical value of the condensation process. The time necessary to reach the critical temperature may be quite long (especially in materials containing large pores) and the condensation process becomes unfeasible. In this contribution, we present a mathematical model that reproduces the condensation process of a gas of positronium in porous silica. It is convenient to divide the condensation dynamics into two parts, according to $t \lessgtr t_c$, where t_c denotes the critical time for the BEC phase transition. The first part ($t < t_c$) includes the cooling of the gas trapped inside the pore in the absence of the condensate. The second part of the process ($t > t_c$) starts when the condensate is beginning to form.

We assume that the gas is constituted by a single population of ortho-positronium. This can be obtained by using a spin-polarized gas of positron in the process of positronium formation. Some radioactive materials (typically ^{22}Na) are a

natural source of spin-polarized positrons. These materials emit highly energetic positrons with a certain spin polarization. The polarization of the positrons can be maintained during all the process of the formation of the positronium atom. However, also in this case, the initial spin polarization of the positronium gas cannot exceed the 30%. Several reactions arise and modify the total lifetime of a positronium gas made of a statistical mixture of spin-up and spin-down atoms. The most important process is the suppression of the minority spin atoms by annihilation with the same amount of atoms with opposite spin. As a result, only a fully spin-polarized ortho-positronium population remains in the gas. The preparation of a highly spin-polarized (96%) ortho-positronium gas trapped in a porous material has been achieved by the group of Cassidy *et al*. [3].

II. POSITRONIUM THERMALIZATION

Let us first examine the gas dynamics for $t < t_c$. Various experiments indicate that the emission energy is in the range of 0.4–3 eV [14,15]. These values seem to be quite independent from the initial kinetic energy of the positron beam. The thermal energy of the positronium is transferred to the pore surface. The dominant relaxation mechanism during the first part of the dynamics is the excitation of phonon modes at the pore surface. Since the positronium is a neutral atom, it interacts with the solid via the acoustic phonon modes. So far, an exhaustive study of the positronium-surface interaction is still lacking. The experiments described in [16,17] showed that the interaction of the positronium in silica with the polar optical phonons is very weak (practically negligible). We simulate the evolution of the temperature of the positronium gas by taking into account the production of acoustic phonons at the pore surface.

We denote by f the positronium distribution function. The evolution of the atomic density inside the cavity is described by the following Boltzmann equation:

$$\begin{aligned}\frac{\partial f}{\partial t} - \frac{\mathbf{p}}{2m}\cdot\nabla_{\mathbf{r}} f &= c\int\{[1+f(\mathbf{p})][1+f(\mathbf{p}_1)]f(\mathbf{p}_2)f(\mathbf{p}_3)\\ &\quad - f(\mathbf{p})f(\mathbf{p}_1)[1+f(\mathbf{p}_2)][1+f(\mathbf{p}_3)]\}\\ &\quad\times\delta(E(\mathbf{p})+E(\mathbf{p}_1)-E(\mathbf{p}_2)-E(\mathbf{p}_3))\\ &\quad\times\delta(\mathbf{p}+\mathbf{p}_1-\mathbf{p}_2-\mathbf{p}_3)d\mathbf{p}_1 d\mathbf{p}_2 d\mathbf{p}_3 - \frac{f}{\tau_p}. \qquad (1)\end{aligned}$$

Here τ_p is the ortho-positronium lifetime (see [18] for the measurement of the ortho-positronium lifetime in a cavity), m denotes the mass of the electron, $c = \frac{2g^2}{(2\pi)^5\hbar^4}$, and $E(\mathbf{p}) = \frac{\mathbf{p}^2}{4m}$. Equation (1) describes the biatomic scattering processes where two atoms undergo to a short-range, hard-sphere, collision. The collision strength is $g = 4\pi\hbar^2 a/m$, where $a = 0.16$ nm is the scattering length [19,20]. The factors $1+f$ in the formula take into account the bosonic nature of the positronium. Finally, the presence in the integral of the two Dirac's δ distributions ensures the conservation of the total energy and momentum during each scattering event.

In proximity of the pore surface, of the positronium atoms interact with the acoustic phonons of the silica. We model the acoustic phonon branch by the linear dispersion relationship $\hbar\omega = v_s q$, where $\hbar\omega$ is the phonon energy, v_s is the sound velocity in silica (around 4900 m/s [21]), and q is the phonon momentum. At the boundary, the interaction of the gas with the cavity surface is described by the equation

$$\left.\frac{\partial f}{\partial t}\right|_{ph\text{-}Ps} = \left.\frac{\partial f}{\partial t}\right|_{Ab} + \left.\frac{\partial f}{\partial t}\right|_{Em},$$

where the first (second) term describes the phonon absorbtion (emission) process. Explicitly,

$$\begin{aligned}\left.\frac{\partial f}{\partial t}\right|_{Ab} &= \frac{1}{4\pi^2\hbar^4}\int S\,\hbar\omega\,\delta(E(\mathbf{p}_1)-E(\mathbf{p})+\hbar\omega)\\ &\quad\times\{[g(\mathbf{p}-\mathbf{p}_1)+1][1+f(\mathbf{p})]f(\mathbf{p}_1)\\ &\quad - g(\mathbf{p}-\mathbf{p}_1)[1+f(\mathbf{p}_1)]f(\mathbf{p})\}d\mathbf{p}_1, \qquad (2)\end{aligned}$$

$$\begin{aligned}\left.\frac{\partial f}{\partial t}\right|_{Em} &= \frac{1}{4\pi^2\hbar^4}\int S\,\hbar\omega\,\delta(E(\mathbf{p}_1)-E(\mathbf{p})-\hbar\omega)\\ &\quad\times\{g(\mathbf{p}-\mathbf{p}_1)[1+f(\mathbf{p})]f(\mathbf{p}_1)\\ &\quad - [g(\mathbf{p}-\mathbf{p}_1)+1][1+f(\mathbf{p}_1)]f(\mathbf{p})\}d\mathbf{p}_1, \qquad (3)\end{aligned}$$

where we defined the transition probability

$$S = \frac{D^2}{v_s^2 M}. \qquad (4)$$

The details of the derivation of Eqs. (2) and (3) can be found in Refs. [22,23]. We defined M as the effective mass of the silica atoms at the interface (around 25 a.m.u. [24]) and D as the deformation potential. In particular, the value $D = 3.6 \pm 0.7$ eV was estimated by Nagai *et al*. by measuring the temperature broadening of the positronium in silica [17]. They found a good agreement between the experimental data and the prediction of a theoretical model in a large range of temperatures (from 88 K to 701 K). In the experiments described in [17], the wave function of the positronium was a Bloch state of the crystal. As a result, the value of the deformation potential is related to the interaction of the positronium with the bulk silica. We expect that the bulk phonon branches could be modified at the pore surface. By using Eq. (4) we obtain $S = 2.1$ eV. The scattering rate S describes the strength of the atom-wall interaction. This is an important parameter for the estimation of the cooling process of the positronium and consequently the formation of the condensate. In order to obtain a better estimation of S, we deduced the value of S by fitting the experimental data of the positronium thermalization presented in [8,9,25]. We obtain S in the interval $[S_0, S_1]$, where $S_0 = 2.6$ eV and $S_1 = 9.1$ eV. In Fig. 1 we plot the evolution of the temperature of the positronium gas contained in a spherical pore of radius 100 nm (left panel) and 300 nm (right panel). The two curves have been obtained using the two extreme values of S. The simulations indicate that the time necessary to reach the temperature of 100 K lies in the interval 7–13 ns for $R = 100$ nm and 20–70 ns for $R = 300$ nm. For large pores, the choice of S becomes critical for deciding if the BEC may be attained. The time necessary to reach the critical temperature may be comparable

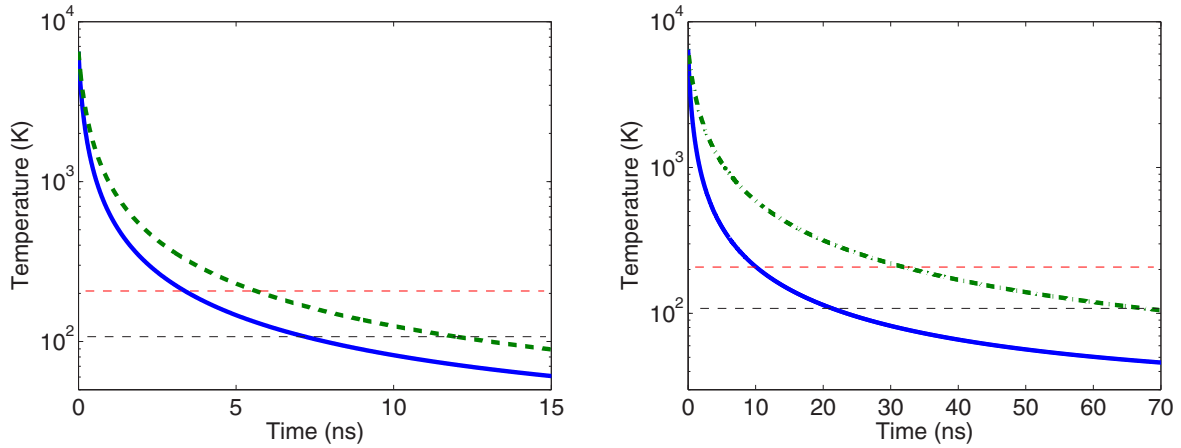

FIG. 1. (Color online) Time evolution of the mean temperature of the positronium gas (the vertical axes are in logarithmic scale) for $t < t_c$, $R = 100$ nm (left panel) and $R = 300$ nm (right panel). Continuous blue curve, $S = S_0$; dashed green curve, $S = S_1$. As a guide for eye, the horizontal dotted black (red) line represents the temperature of 100 (200) K.

with the lifetime of the ortho-positronium. In our simulations of the condensation dynamics we use the value $S = 4.5$ eV. According to [8], in our simulations we assumed that the positronium atoms are emitted by the pore surface into the cavity with an initial energy of 0.56 eV. In the case of higher injection energies (2 eV) the results are only slightly modified. Indeed, we have observed that during the first stage of the thermalization process ($t < 1$ ns), the temperature of the Ps decreases very fast and the value of 0.5 eV is reached in less than 2.5 ns (pore size 100 nm).

III. CONDENSATION DYNAMICS: EVOLUTION OF THE NONCONDENSED ATOMS

The second stage of the dynamics ($t > t_c$) is characterized by the production of the condensate. Special care is required for modeling the interaction among the low-energy positronium atoms in this supercritical regime. While the thermalization dynamics is essentially a classical mechanism of energy transfer among particles and surfaces, the production of a condensate is intrinsically a quantum-mechanical phenomenon.

We simulate the evolution of the condensed phase and the noncondensed particles by the quantum-kinetic formalism. The quantum-kinetic formalism constitutes a fully quantum framework that displays strong analogies with the classical phase-space description of a statistical system based on the Boltzmann evolution equation. We describe the condensation dynamic of the positronium by combining the quantum-kinetic formalism with the Bogoliubov-Popov description of the pseudoparticles. The collision processes are obtained by applying the Baliev many-particle theory [26].

The many-body Hamiltonian describing interacting bosons is given by (see, for example, [27,28])

$$K = \int \psi^\dagger(\mathbf{r}) \left[-\frac{\Delta}{2m} - \mu \right] \psi(\mathbf{r}) d\mathbf{r} + \frac{g}{2} \int \psi^\dagger(\mathbf{r}) \psi^\dagger(\mathbf{r}) \psi(\mathbf{r}) \psi(\mathbf{r}) d\mathbf{r},$$

where ψ ($\psi^\dagger$) denotes the creation (annihilation) operator of the bosons and μ the chemical potential. The elementary particle-particle scattering event is modeled by the hard-sphere interaction with collision strength $g = 4\pi\hbar^2 a/m$.

In order to develop the convenient mathematical formulation of the problem, it is customary to distinguish between the particles that form the condensate and the surrounding gas (the noncondensed cloud). This is technically achieved by defining the field $\widetilde{\psi} = \psi - \langle\psi\rangle$ (similar definition for $\widetilde{\psi}^\dagger$), where ψ is the positronium annihilation operator, $\langle\psi\rangle = \Phi$ is the macroscopic wave function of the condensate (usually referred to as the order parameter), and the brackets $\langle\cdot\rangle$ denote the expectation value. In particular, the squared modulus of the order parameter gives the density of condensed particles $n_c = |\Phi|^2$.

The presence of a condensed phase induces strong correlations among particles with small momenta. In contrast to a normal system, in the presence of a condensed phase, the expectation values of operators that do not conserve the total number of particles—such as, for example, $\langle\widetilde{\psi}\widetilde{\psi}\rangle$ and $\langle\widetilde{\psi}^\dagger\widetilde{\psi}^\dagger\rangle$—are no longer zero. This leads to new type of atomic interaction, generally denoted as "anomalous" scattering processes. They describe the exchange of particles between the condensate and the surrounding noncondensed gas. The many-particle system is described by the Green's function [29,30]

$$\widehat{\mathcal{G}}(\mathbf{r},\mathbf{r}';t,t') = -iT\{\Psi(\mathbf{r},t)[\Psi^\dagger(\mathbf{r}',t')]^t\}, \tag{5}$$

where T denotes the temporal ordering operator and $\Psi = \begin{pmatrix} \widetilde{\psi} \\ \widetilde{\psi}^\dagger \end{pmatrix}$. A convenient description of the noncondensed particles is obtained by the so-called Wigner-transformed Green's function

$$\mathcal{G}(\mathbf{r},\mathbf{p};t,\omega) \equiv \frac{1}{(2\pi)^4} \int \widehat{\mathcal{G}}\left(\mathbf{r} + \frac{\hbar\boldsymbol{\eta}}{2}, t + \frac{\hbar\tau}{2}; \mathbf{r} - \frac{\hbar\boldsymbol{\eta}}{2}, t - \frac{\hbar\tau}{2}\right) \times e^{-i(\mathbf{p}\boldsymbol{\eta} - \tau\omega)} d\boldsymbol{\eta} d\tau. \tag{6}$$

The function $\mathcal{G}(\mathbf{r},\mathbf{p};t,\omega)$ is a 2×2 matrix whose variables are the mean position $\mathbf{r}$, the momentum $\mathbf{p}$, the mean time t, and the energy variable ω. By analogy with the description of a classical gas, the noncondensed cloud is described by a distribution density function $f(\mathbf{r},\mathbf{p},t)$ (Wigner function). The

positronium distribution function $f(\mathbf{r},\mathbf{p},t)$ is obtained by the classical limit

$$f(\mathbf{r},\mathbf{p},t) = i \lim_{\hbar\to 0} \mathrm{tr}\langle\widehat{\mathcal{G}}^{<}\rangle, \tag{7}$$

where tr denotes the trace and $<$ the less-than function. The function f provides the number of atoms of positronium at the position $\mathbf{r}$ with momentum $\mathbf{p}$. The evolution equation for the positronium distribution has a Boltzmann-like form,

$$\frac{\partial f}{\partial t} - \nabla_{\mathbf{r}}\mathfrak{E}\cdot\nabla_{\mathbf{p}} f + \nabla_{\mathbf{p}}\mathfrak{E}\cdot\nabla_{\mathbf{p}} f = -\frac{f}{\tau_p} + \frac{1}{\hbar}\int \mathrm{tr}\{\Sigma^{>}\langle\widehat{\mathcal{G}}^{<}\rangle - \Sigma^{<}\langle\widehat{\mathcal{G}}^{>}\rangle\}d\omega, \tag{8}$$

where $\mathfrak{E}$ denotes the Bogoliubov spectrum $\mathfrak{E} = \sqrt{\mathfrak{e}^2 - g^2 n_c^2}$, $\mathfrak{e} = \frac{\mathbf{p}^2}{4m} - \mu + 2gn_c$, and n_c is the condensate density. Furthermore, Σ denotes the positronium self-energy operator. It describes the collisions among noncondensed particles and the collisions involving condensed and noncondensed particles. The derivation of Eq. (8) is given in detail in Ref. [31].

The physics of the interaction of a many-particle boson gas has been thoroughly investigated (see, for example, [29,32]). A sophisticated instrument for the analysis of the many-body boson scattering process is provided by the Baliev theory [26] (see, for example, [33,34] for a clear review of the main results of the theory). We apply the Baliev-Popov theory and we include in our model the main Hartree-Fock-Bogoliubov scattering processes in the gapless approximation. The related Feynman diagrams can be found, for example, in Ref. [29]. The calculations are discussed in Ref [31]. As a final result, we obtain

$$\frac{1}{\hbar}\int \mathrm{tr}\{\Sigma^{>}\langle\widehat{\mathcal{G}}^{<}\rangle - \Sigma^{<}\langle\widehat{\mathcal{G}}^{>}\rangle\}d\omega = \mathcal{W}_{\mathrm{HF}} + \mathcal{W}_{\mathrm{cn}}, \tag{9}$$

where

$$\mathcal{W}_{\mathrm{HF}} = \frac{2g^2}{(2\pi)^5\hbar^7}\int \delta(\mathfrak{E}+\mathfrak{E}_1-\mathfrak{E}_2-\mathfrak{E}_3) \times \delta(\mathbf{p}+\mathbf{p}_1-\mathbf{p}_2-\mathbf{p}_3)\,[(f+1)(f_1+1) \times f_2 f_3 - f f_1 (f_2+1)(f_3+1)]\mathsf{T}_{\mathrm{HF}} d\mathbf{p}_1 d\mathbf{p}_2 d\mathbf{p}_3, \tag{10}$$

$$\mathcal{W}_{\mathrm{cn}} = \frac{2g^2}{(2\pi)^2\hbar^4}\int \mathsf{T}_{\mathrm{nc}}\,[(1+f_1)\,f_2 f_3 - f_1\,(1+f_2)\,(1+f_3)] \times [\delta(\mathbf{p}-\mathbf{p}_1) - \delta(\mathbf{p}-\mathbf{p}_2) - \delta(\mathbf{p}-\mathbf{p}_3)] \times \delta(\mathbf{p}_1-\mathbf{p}_2-\mathbf{p}_3)\,\delta(\mathfrak{E}_1-\mathfrak{E}_2-\mathfrak{E}_3)\,d\mathbf{p}_1 d\mathbf{p}_2 d\mathbf{p}_3\,. \tag{11}$$

The scattering kernels are given by the following expressions:

$$\mathsf{T}_{\mathrm{cn}} = (u_1u_2u_3 + v_1v_2v_3 + u_1v_2v_3 + v_1u_2v_3 - u_1v_2u_3 - v_1u_2u_3)^2, \tag{12}$$
$$\mathsf{T}_{\mathrm{HF}} = (u_p u_1 u_2 u_3 + v_p u_1 v_2 u_3 + v_p u_1 u_2 v_3 + v_p v_1 v_2 u_3 + u_p v_1 v_2 v_3)^2.$$

In order to simplify the notations, we defined $\mathfrak{E}_i \equiv \mathfrak{E}(\mathbf{p}_i)$, $\mathfrak{E} \equiv \mathfrak{E}(\mathbf{p})$, $f_i \equiv f(\mathbf{p}_i)$, $f \equiv f(\mathbf{p})$, $c = \frac{g^2}{2(2\pi)^2}$, and $u = \sqrt{\frac{\mathfrak{e}+\mathfrak{E}}{2\mathfrak{E}}}$, $v = \sqrt{\frac{\mathfrak{e}-\mathfrak{E}}{2\mathfrak{E}}}$. This model has been successfully used for the simulation of the condensation dynamics of a gas of sodium [31]. The collision kernels $\mathcal{W}_{\mathrm{HF}}$ and $\mathcal{W}_{\mathrm{cn}}$ are derived in the framework of the boson interaction theory of Baliev [26] (see, for example, [33,34] for a clear review of the main results of the theory). The term $\mathcal{W}_{\mathrm{HF}}$ describes the binary collisions between noncondensed particles and $\mathcal{W}_{\mathrm{cn}}$ takes into account all the scattering processes where only one condensed particle is involved. As an example, $\mathcal{W}_{\mathrm{cn}}$ describes transitions where one particle is injected in the condensate after a collision with another noncondensed particle or where one atom is expelled from the condensate by a collision with the surrounding noncondensed cloud. The particle interactions are described by the scattering rates T_{HF} and T_{cn}. They have a complex form and depend nonlinearly on the density of the condensed particles n_c. Similar expressions of the collision rates between condensed and noncondensed particles were obtained in [30,35]. It is easy to verify that Eq. (8) coincides with Eq. (1) when $n_c = 0$. In fact, in this case $\mathfrak{e} = \mathfrak{E} = E = \frac{p^2}{4m}$, $\mathsf{T}_{\mathrm{HF}} = 1$, and $\mathcal{W}_{\mathrm{cn}} = 0$. A kinetic model similar to Eq. (9) was considered for the study of the dynamics and the relaxation time of the condensate excitations [36]. In their approach, the authors considered only the bare hard-sphere interaction and discarded the modification of the scattering rate induced by the presence of the condensate (in our model this is obtained by setting $\mathsf{T}_{\mathrm{HF}} = \mathsf{T}_{\mathrm{cn}} = 1$). This is justified only for a hot cloud of noncondensed particles and is no longer accurate when the gas reaches the critical temperature.

IV. CONDENSATE EVOLUTION

The Bose-Einstein condensation process corresponds to a spontaneous breaking of a U(1) symmetry where the excitation spectra displays a Goldstone branch without energy gap in the long-wavelength limit. The condensate atoms are described by the order parameter $\Phi = \langle\psi\rangle$. The evolution equation of Φ is given by the so-called Gross-Pitaevskii (GP) equation. The GP equation describes the evolution of the condensate in the presence of the Hartree mean field produced by the atoms. Zaremba and co-workers showed that the Boltzmann-like approach (8) is compatible with the GP equation, provided that a non-Hermitian term is inserted in the equation for the order parameter [37]. As a result, the GP equation that describes the evolution of the BEC interacting with a noncondensed cloud is given by [29]

$$i\hbar\frac{\partial\Phi(\mathbf{r},t)}{\partial t} = \left[-\frac{\hbar^2\Delta_{\mathbf{r}}}{2m} + g\,|\Phi(\mathbf{r},t)|^2 + 2gn(\mathbf{r},t) - \frac{i\hbar}{2\tau_p} - \frac{i}{n_c}\int \mathcal{W}_{\mathrm{cn}}(\mathbf{p})d\mathbf{p}\right]\Phi(\mathbf{r},t), \tag{13}$$

where n is the density of the noncondensed positronium defined as

$$n = \frac{1}{(2\pi)^3}\int f(\mathbf{p})d\mathbf{p}. \tag{14}$$

The stationary solution is obtained by the standard substitution $i\hbar\frac{\partial\Phi(\mathbf{r},t)}{\partial t} \to \mu\Phi$. Several methods have been proposed for the numerical implementation of the GP equation [38]. Numerical schemes for the solution of the GP equation in spherically

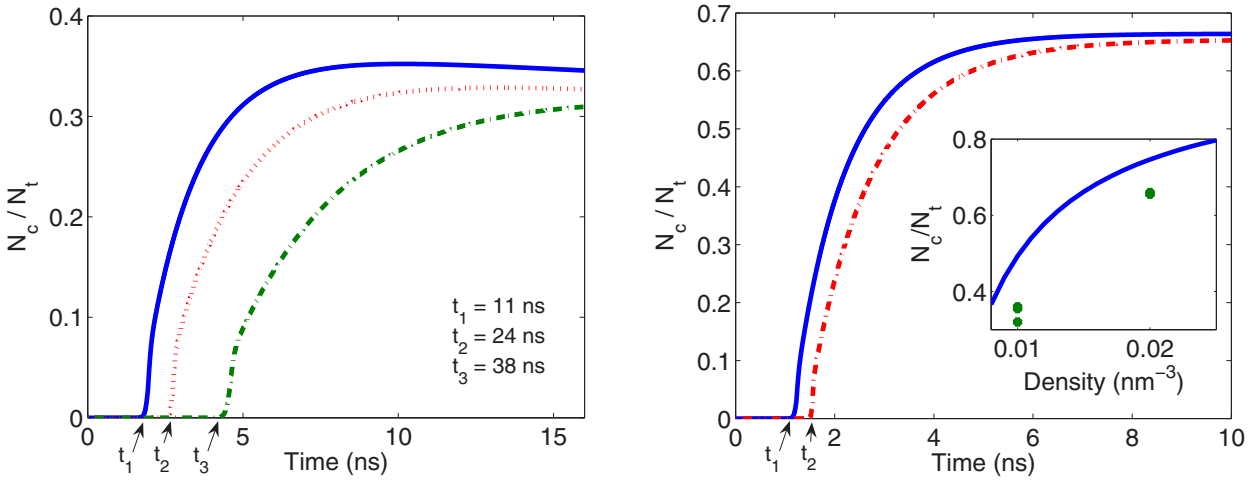

FIG. 2. (Color online) Time evolution of the ratio between condensed N_c and total number of particles N_t. (Left panel) Particle density 10^{-2} nm^{-3} ($T_c = 66$ K). Pore sizes: $R = 100$ nm (continuous blue curve), $R = 200$ nm (dashed red curve), $R = 300$ nm (dot-dashed green curve). Total condensation time: $t_1 = 11$ ns, $t_2 = 24$ ns, $t_3 = 38$ ns. (Right panel) Particle density 2×10^{-2} nm^{-3} ($T_c = 105$ K). Pore sizes: $R = 100$ nm (continuous blue curve) and $R = 200$ nm (dashed red curve). Critical condensation times: $t_1 = 5$ ns, $t_2 = 19$ ns. (Right panel, inset) Condensate density for a uniform system (continuous curve) and final values obtained with the numerical simulations (dots).

symmetric systems are described in [39]. The link between the condensed and noncondensed atoms is expressed by the term $\mathcal{W}_{\rm cn}$. It can be easily understood in terms of a balance of particles. Since the total number of particles is conserved, the last term of Eq. (13) takes into account the transitions of the atoms between the condensed and the noncondensed systems [40]. In particular, the integral of the scattering rate $\mathcal{W}_{\rm cn}$ over the momentum provides the rate at which the particles enter or leave the condensate [40]. We have

$$\frac{dN_c}{dt} = \frac{d}{dt}\int |\Phi(\mathbf{r})|^2\, d\mathbf{r} = \int \mathcal{W}_{\rm cn} d\mathbf{p} d\mathbf{r} - \frac{N_c}{\tau_p}, \qquad (15)$$

where N_c is the total number of atoms in the condensate.

Equations (9) and (13) describe the interaction between condensed and noncondensed particles. Dynamical models based on the Boltzmann formalism have been applied to the study of the evolution and thermalization processes of a gas in the supercritical regime by Gardinier *et al.* [41] and Zaremba *et al.* [42]. Numerical approaches where the Boltzmann dynamics is coupled with the GP equation also exist (see, for example, [40] and citations therein).

In our formulation, the condensate is treated in a fully quantum-mechanical context and its correlation with the surrounding thermal cloud is addressed explicitly. The presence of the condensate alters considerably the simple hard-sphere scattering process that characterizes the bare positronium. In particular, the use of the correct Bogoliubov representation for atoms with a small mass (like the atom of positronium) leads to a significant modification of the condensate evolution. Furthermore, the use of the quasiparticle spectrum has the advantage that the modification of the energy levels induced by the presence of the condensate is automatically taken into account. The main difficulty for the numerical resolution of the coupled Boltzmann-GP system arises from the presence of a nonlinearity in the collision kernel and the divergence of the distribution function at $\mathbf{p} = 0$. The latter is intrinsically related to the Bose-Einstein condensation mechanism. These points were addressed in Ref. [31].

We solved numerically Eq. (9) together with Eq. (13). The process of condensation is summarized in Figs. 2–5. In Fig. 2 we plot the evolution of the ratio between the condensed atoms $N_c = \int |\Phi|^2\, d\mathbf{r}$ and the total number of positronium inside the pore, for different pore sizes. In the plots of Fig. 2, we set the origin of the time axis at the time when the gas temperature has reached 100 K (left panel) or 200 K (right panel). The total time elapsed from the particle injection until the beginning of the condensation (critical time t_c) is indicated in the caption of the figure. The temperature of the pore surface is set to 30 K. The simulations show that the condensation process requires around 10–20 ns. This time is typically shorter than the time necessary for cooling the gas to the critical temperature t_c. Our

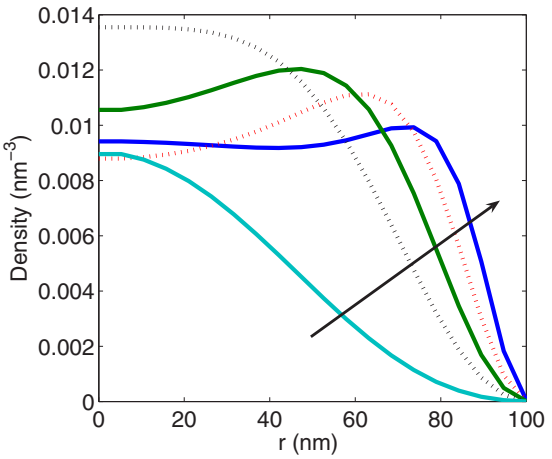

FIG. 3. (Color online) (Left panel) Density profile of the BEC for different times after the beginning of the condensation process: 0.2 ns (light blue continuous line), 0.8 ns (black dotted line), 2 ns (green continuous line), 3 ns (red dotted line), and 5 ns (blue continuous line). Here $R = 100$ nm and the arrow indicates the time direction.

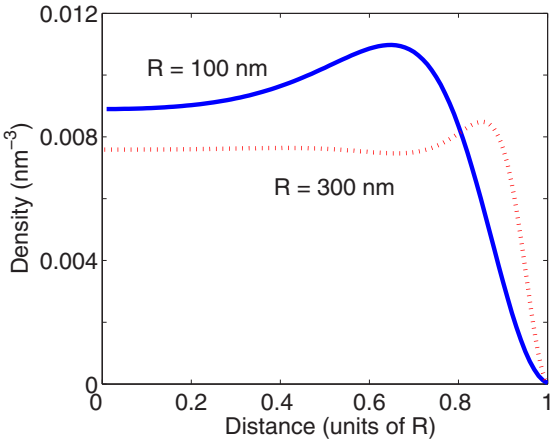

FIG. 4. (Color online) Comparison of the condensate density profile for different cavity radii: $R = 100$ nm (blue continuous line), $R = 300$ nm (red dotted line). The horizontal axis is in units of the cavity radius R.

results show that the condensation dynamics of positronium is qualitatively similar to the analogous process for excitons [43] and polaritons [44]. One interesting difference is encountered in the first part of the dynamics. The initial growth of the exciton condensate proceeds smoothly, whereas similarly to what is presented in [44,45] for polaritons, our simulations show a fast initial increase of the condensate density. The process responsible for the cooling of the particles and the subsequent condensation is, however, quite different. In the case of excitons or polaritons, the role of the pore surface is played by a thermal phonon bath, which constitutes a uniform reservoir of particles maintained at a temperature below the critical value.

The evolution of the condensate density profile is depicted in Fig. 3. The shape of the condensate density differs from the typical Gaussian profile obtained in a harmonic trap. The inhomogeneity of the condensed density profile has an interesting consequence: The simulations show the presence of a flux of particles entering the condensate near the boundary and a corresponding flux of particles leaving the condensate at the center. Close to the surface, the temperature of the gas and the condensate density are small. This condition makes the condensate production rather efficient. The condensate particles accumulate around the center of the cavity, where the noncondensed gas is hotter. In this region, the balance between condensate and noncondensate particles is unfavorable to the condensation process and some particles leave the condensate. This in-out flux of particles limits the condensate production in the early stages of the condensation process. Figure 3 shows clearly that the quantum confinement of the condensate affects the final shape of the density up to a distance of nearly 30 nm from the pore surface.

When the condensate density increases, the particles are more uniformly distributed and occupy the whole cavity. In Fig. 4 we compare the final density distribution of the condensed particles inside the cavity for two different values of the pore radius (100 and 300 nm). The simulations show that the final condensate distribution in large cavities is nearly uniform and the value of the density of the condensate is not very sensitive to the radius of the cavity.

For the sake of comparison, in Fig. 2 (inset of the right panel) we depict the theoretical value of the ratio of the condensed and total density of a uniform gas given by $\frac{N_c}{N_t} = 1 - (T_b/T_c)^{3/2}$, where T_b is the bulk temperature, $T_c = \frac{\pi N_t^{2/3}}{2mk_B}$ is the critical temperature of the gas, and k_B is the Boltzmann constant [27]. The final values of the condensed density obtained with our simulations are indicated with a dot. They show a good agreement with the theoretical values.

In Fig. 5 (left panel) we represent the total time (starting from the injection of the hot Ps gas in the pore) necessary to reach 90% of condensed particles for different cavity sizes. The total number of particles in the condensate is shown in the right panel. The results demonstrate that the condensation time is compatible with the lifetime of ortho-positronium and suggest that a pore size of around 200 nm could be a good compromise between short condensation time and a large number of particles in the condensate. At the density of 10^{-2} nm^{-3}, the number of atoms in the condensate is limited to around 10^6. When the volume of the pore increases, an

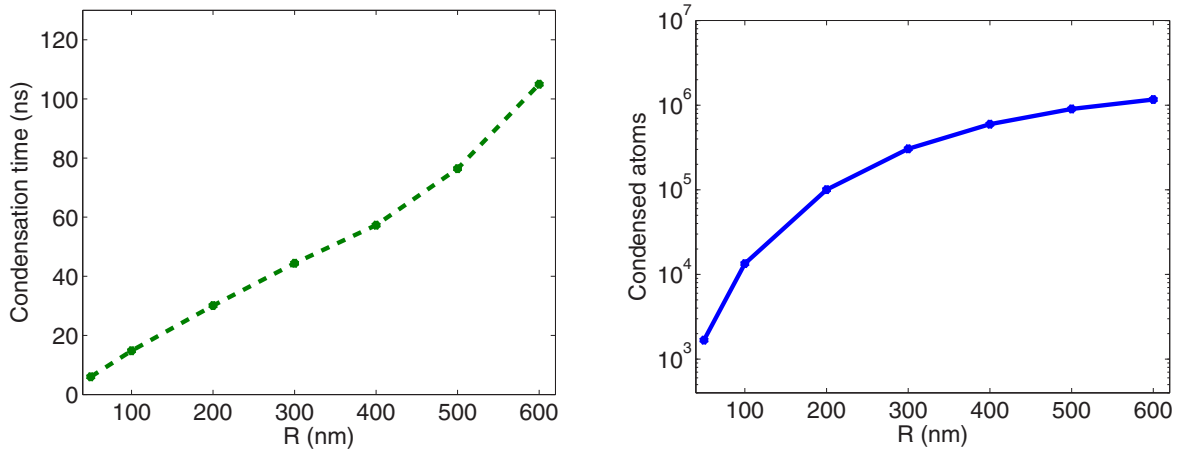

FIG. 5. (Color online) (Left panel) Total time necessary to reach 90% of the condensed particles for different pore sizes. (Right panel) Maximum number of condensed particles. Particle density: 10^{-2} nm^{-3}.

increasing number of particles annihilate before entering the condensate. For pores with size below 100 nm the number of atoms in the condensate could be too small. Moreover, as indicated in Fig. 1, the uncertainty on the knowledge of the particle-wall interaction potential compromises the accuracy of the results of our model for very large pores ($R > 300$ nm).

V. CONCLUSION

In summary, within the framework of a multiscale modeling and a quantum-kinetic approach, our numerical simulations reveal that, under realistic conditions, the Bose-Einstein condensation process of a positronium gas could be observed within the lifetime of ortho-positronium, even without resorting to extremely low temperatures (the silica substrate is maintained at 30 K). Thus, depending on the initial particle density, it is possible to reach the condensation of a significative fraction of the total number of positronium atoms initially injected into the cavity.

ACKNOWLEDGMENTS

This work was partially funded by the Agence Nationale de la Recherche (Contract No. ANR-10-BLAN-0420). We thank P. Perez and L. Liszkay for many interesting discussions.

[1] D. B. Cassidy and A. P. Mills, Phys. Stat. Sol. **4**, 3419 (2007).
[2] P. M. Platzman and A. P. Mills, Phys. Rev. B **49**, 454 (1994).
[3] D. B. Cassidy, V. E. Meligne, and A. P. Mills, Phys. Rev. Lett. **104**, 173401 (2010).
[4] P. Perez (private communication).
[5] D. B. Cassidy, S. H. M. Deng, R. G. Greaves, T. Maruo, N. Nishiyama, J. B. Snyder, H. K. M. Tanaka, and A. P. Mills, Phys. Rev. Lett. **95**, 195006 (2005).
[6] D. B. Cassidy, T. H. Hisakado, H. W. K. Tom, and A. P. Mills, Phys. Rev. Lett. **108**, 043401 (2012).
[7] D. B. Cassidy and A. P. Mills, Nature (London) **449**, 195 (2007).
[8] S. Takada, T. Iwata, K. Kawashima, H. Saito, Y. Nagashima, and T. Hyodo, Radiat. Phys. Chem. (UK) **58**, 781 (2000).
[9] T. Chang, M. Xu, and X. Zeng, Phys. Lett. A **126**, 189 (1987).
[10] R. F. Kiefl and D. R. Harshman, Phys. Lett. A **98**, 447 (1983).
[11] D. B. Cassidy, P. Crivelli, T. H. Hisakado, L. Liszkay, V. E. Meligne, P. Perez, H. W. K. Tom, and A. P. Mills, Jr., Phys. Rev. A **81**, 012715 (2010).
[12] S. Mariazzi, A. Salemi, and R. S. Brusa, Phys. Rev. B **78**, 085428 (2008).
[13] S. Mariazzi, P. Bettotti, and R. S. Brusa, Phys. Rev. Lett. **104**, 243401 (2010).
[14] P. Sferlazzo, S. Berko, and K. F. Canter, Phys. Rev. B **35**, 5315 (1987).
[15] Y. Nagashima, Y. Morinaka, T. Kurihara, Y. Nagai, T. Hyodo, T. Shidara, and K. Nakahara, Phys. Rev. B **58**, 12676 (1998).
[16] I. V. Bondarev, Y. Nagai, M. Kakimoto, and T. Hyodo, Phys. Rev. B **72**, 012303 (2005).
[17] Y. Nagai, M. Kakimoto, T. Hyodo, K. Fujiwara, H. Ikari, M. Eldrup, and A. T. Stewart, Phys. Rev. B **62**, 5531 (2000).
[18] D. W. Gidley, W. E. Frieze, T. L. Dull, A. F. Yee, E. T. Ryan, and H.-M. Ho, Phys. Rev. B **60**, R5157 (1999).
[19] O. Kenji, T. Miyakama, H. Yabu, and T. Suzuki, J. Phys. Soc. Jpn. **70**, 1549 (2001).
[20] I. A. Ivanov, J. Mitroy, and K. Varga, Phys. Rev. A **65**, 022704 (2002).
[21] R. Vacher and J. Pelous, Phys. Rev. B **14**, 823 (1976).
[22] M. Galler and F. Schürrer, J. Phys. A: Math. Gen. **37**, 1479 (2004).
[23] J. M. Ziman, *Electrons and Phonons* (Clarendon, Oxford, UK, 2001).
[24] C. He, M. Muramatsu, N. Oshima, T. Ohdaira, A. Kinomura, and R. Suzuki, Phys. Lett. A **355**, 73 (2006).
[25] Y. Nagashima, T. Hyodoy, K. Fujiwarayx, and A. Ichimuraz, J. Phys. B: At. Mol. Opt. Phys. **31**, 329 (1998).
[26] S. T. Beliaev, Sov. Phys. JETP **7**, 289 (1958).
[27] A. L. Fetter, J. Low Temp. Phys. **129**, 263 (2002).
[28] H. Shi and A. Griffin, Phys. Rep. **304**, 1 (1998).
[29] A. Griffin, T. Nikuni, and E. Zaremba, *Bose Condensed Gases at Finite Temperatures* (Cambridge University Press, Cambridge, UK, 2009).
[30] T. R. Kirkpatrick and J. R. Dorfman, Phys. Rev. A **28**, 2576 (1983).
[31] O. Morandi, P.-A. Hervieux, and G. Manfredi, Phys. Rev. A **88**, 023618 (2013).
[32] S. A. Moskalenko and D. W. Snoke, *Bose-Einstein Condensation of Excitons and Biexcitons: And Coherent Nonlinear Optics with Excitons* (Cambridge University Press, Cambridge, U.K., 2000).
[33] B. Capogrosso-Sansone, S. Giorgini, S. Pilati, L. Pollet, N. Prokof'ev, B. Svistunov, and M. Troyer, New J. Phys. **12**, 043010 (2010).
[34] L. P. Pitaevskii and S. Stringari, *Bose-Einstein Condensation* (Oxford University Press, Oxford, U.K., 2003).
[35] M. Imamovic-Tomasovic and A. Griffin, J. Low Temp. Phys. **122**, 617 (2001).
[36] J. E. Williams and A. Griffin, Phys. Rev. A **64**, 013606 (2001).
[37] E. Zaremba, T. Nikuni, and A. Griffin, J. Low Temp. Phys. **116**, 277 (1999).
[38] W. Bao, D. Jaksch, and P. A. Markowich, J. Comput. Phys. **187**, 318 (2003).
[39] M. Edwards and K. Burnett, Phys. Rev. A **51**, 1382 (1995).
[40] B. Jackson and E. Zaremba, Phys. Rev. A. **66**, 033606 (2002).
[41] C. W. Gardiner, M. D. Lee, R. J. Ballagh, M. J. Davis, and P. Zoller, Phys. Rev. Lett. **81**, 5266 (1998).
[42] M. J. Bijlsma, E. Zaremba, and H. T. C. Stoof, Phys. Rev. A **62**, 063609 (2000).
[43] L. Banyai, P. Gartner, O. M. Schmitt, and H. Haug, Phys. Rev. B **61**, 8823 (2000).
[44] H. T. Cao, T. D. Doan, D. B. Tran Thoai, and H. Haug, Phys. Rev. B **69**, 245325 (2004).
[45] D. Porras, C. Ciuti, J. J. Baumberg, and C. Tejedor, Phys. Rev. B **66**, 085304 (2002).